

Supporting information for

A New Highly Sensitive and Selective Fluorescence Chemosensor for Cr³⁺ Based on a Rhodamine B and 4, 13-Diaza-18-Crown 6-Ether Conjugate

Duliang Liu^{a, ‡}, Tao Pang^{b, c, ‡}, kefeng, Ma^a, Wei Jiang^a, Xiaofeng Bao^{a, *}

^a Department of Biochemical Engineering, Nanjing University of Science & Technology, Chemical Engineering Building B302, 200 Xiaolinwei, Nanjing, P.R.China. E-mail: baoxiaofeng@njust.edu.cn

^b New Drug Screening Center, China Pharmaceutical University, Nanjing, P.R.China.

^c State Key Laboratory of Natural Medicines, China Pharmaceutical University, Nanjing, P.R.China

* E-mail: baoxiaofeng@mail.njust.edu.cn

Table of Contents

| | |
|---|--------------|
| Experimental Section..... | S3 page |
| Materials and Instruments..... | S3 Page |
| Cell Studies..... | S4 Page |
| Synthesis of compound 5..... | S5 Page |
| Synthesis of compound 7..... | S6 Page |
| ¹ H NMR and ESI-MS spectra of compound 7..... | S7 Page |
| Synthesis of compound 2..... | S8 Page |
| ¹ H, ¹³ C NMR and ESI-HRMS spectra of compound 2..... | S9,S10 Page |
| Synthesis of compound 1..... | S11,S12 Page |

| | |
|--|--------------|
| ¹ H, ¹³ C NMR and ESI-HRMS spectra of compound 1..... | S12,S13 Page |
| UV-Vis absorbance and fluorescence experiments..... | S13 Page |
| Fluorescence spectra of probe 1 + different amounts of Cr ³⁺ | S14 Page |
| Color change of probe 1 + different amounts of Cr ³⁺ | S15 Page |
| Job's Plot of probe 1 with Cr ³⁺ | S16 Page |
| Determination of the association constant K _a | S17 Page |
| Determination of detection limit..... | S18 Page |
| Color change of probe 1 + various cations..... | S19Page |
| Ratio change of probe 1 with background cations + Cr ³⁺ | S20 Page |
| UV-Vis spectra of probe 1 + various cations..... | S21 Page |
| Comparison of fluorescence spectra of probe 1 with probe 2 + various cations..... | |
| | S22 Page |
| Comparison of Partial ¹ H NMR of probe 1 + Cr ³⁺ with probe 1 without Cr ³⁺ | |
| | S23 Page |
| PH response of probe 1..... | S23 Page |
| Table S1..... | S24 Page |
| Reference..... | S25 Page |

EXPERIMENTAL SECTION

1. Materials and Instruments

All of the reagents and organic solvents were ACS grade or higher and used without further purification. Unless otherwise noted, all of the chemicals were purchased from J&K Scientific (Shanghai, China). The reactions were performed under an argon atmosphere using standard Schlenk techniques. Thin-layer chromatography was performed on a HAIYANG silica gel F254 plate, and the compounds were visualized under UV light ($\lambda = 254$ nm). Column chromatography was performed using HAIYANG silica gel (type: 200–300 mesh ZCX-2). ^1H (500 MHz) and ^{13}C NMR (126 MHz) spectra were recorded on an Avance 500 spectrometer (Bruker; Billerica, MA, USA). The chemical shifts are reported in δ units (ppm) downfield relative to the chemical shift for tetramethylsilane. The following abbreviations were used to represent the multiplicities: s = singlet, d = doublet, t = triplet, q = quartet, m = multiplet, br = broad. Mass spectra were obtained with a Finnigan TSQ Quantum LC/MS Spectrometer.

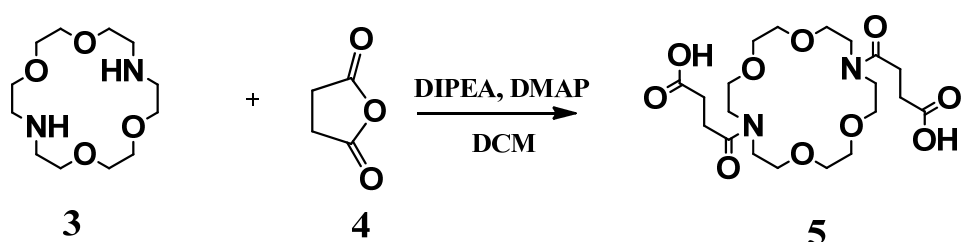
The pH of the stock solution was measured using a PHS-25C Precision pH/mV Meter (Aolilong, Hangzhou, China) and adjusted by adding 10% NaOH. The UV-Vis absorbance and fluorescence spectra were recorded with a UltroSPec 4300 Pro spectrophotometer (Amersham Biosciences, USA) and a Edinburgh FLS920 fluorescence spectrophotometer (Livingston, UK), respectively.

2. Cell Studies

In vitro experiments were performed using human L-02 liver cells. L-02 cells were cultured in RPMI-1640 medium supplemented with 10% fetal bovine serum (FBS) in an atmosphere of 5% CO₂ at 37°C. Cytotoxicity of probe **1** was determined by an MTT assay. Briefly, L-02 hepatocytes were incubated with different concentrations of probe **1** for 24 h. Cell viability was evaluated by incubating with 0.5 mg/ml 3-[4,5-dimethylthiazol-2-yl]-2,5-diphenyltetrazolium bromide (MTT) for 4 h under 5% CO₂/95% air at 37°C. Media were replaced with 100 µL DMSO, and absorbance was read at 570 nM. For fluorescence microscopy images, one day before imaging, L-02 cells were seeded in 6-well plates. Immediately, before the experiments, the L-02 cells were exposed to probe **1** (20 µM) in PBS for 2 h at 37°C to allow the probe to permeate into the cells and supplementing cells with 100 µM CrCl₃ at 37°C under 5% CO₂ for another 1 h. The cells were washed with PBS three times and then imaged. The fluorescence imaging of intracellular was observed under an Olympus inverted fluorescence microscopy with 20× objective lens multiplied by 1.6 (excited with green light). The L-02 cells incubated with solvent DMSO was taken as a control.

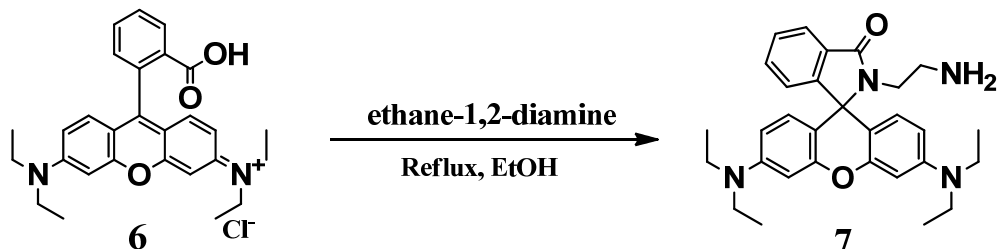
2. Preparation of Compounds

Synthesis of 4,4'-(1,4,10,13-tetraoxa-7,16-diazacyclooctadecane-7,16-diyl)bis-(4-oxobutanoic acid)(5).



To a stirred solution of diaza-18-crown-6 (50 mg, 0.1908 mmol), 4-DMAP (23 mg, 0.1908 mmol, 1.0 eq.) and DIPEA (33 μ L, 1 eq.) in 5 mL of dry DCM, succinic anhydride (42 mg, 0.4198 mmol, 2.2 eq.) was added. Then, the resulting mixture was stirred at room temperature under a nitrogen atmosphere for 20 h. The progress of the reaction was monitored by TLC dyed with iodine vapor. The solvent was removed under reduced pressure to afford a white-oil (crude product) in approximately 100% yield. The crude product was not further purified and treated as a reagent in the next step.

Synthesis of 2-(2-aminoethyl)-3',6'-bis(diethylamino)spiro[isoindoline-1,9'-xanthan]-3-one (7).



To a stirred solution of Rhodamine B (2.2 g, 4.6 mmol) in 30 mL of ethanol, ethane-1,2-diamine (3.1 mL, 10 eq.) was added through needle tubing. The resulting mixture was refluxed under a nitrogen atmosphere overnight. The progress of the reaction was monitored by TLC. After the crude material was concentrated in vacuum to remove the EtOH solvent, the obtained pink residue was purified on a silica gel column with MeOH/CH₂Cl₂ (v:v 1:50 to 1:20) to yield a pink solid (2.1 g, 95% yield).
Rf=0.3 (MeOH/CH₂Cl₂, v:v 1:20); ¹H NMR (500 MHz, CDCl₃, 298 K): δ 7.909-7.891(m, 1H), 7.451-7.434(q, 2H), 7.100-7.082(m, 1H), 6.440-6.422(d, 2H), 6.376-6.371(d, 2H), 6.284-6.261(q, 2H), 3.353-3.309(q, 8H), 3.203-3.177(t, J=6.5 Hz, 2H), 2.432-2.406(t, J=6.5 Hz, 2H), 1.176-1.148(t, J=7.0 Hz, 12H); ESI-MS(m/z): calcd. for [M+1]⁺ C₃₀H₃₇N₄O₂⁺ 485.29, found 485.13.

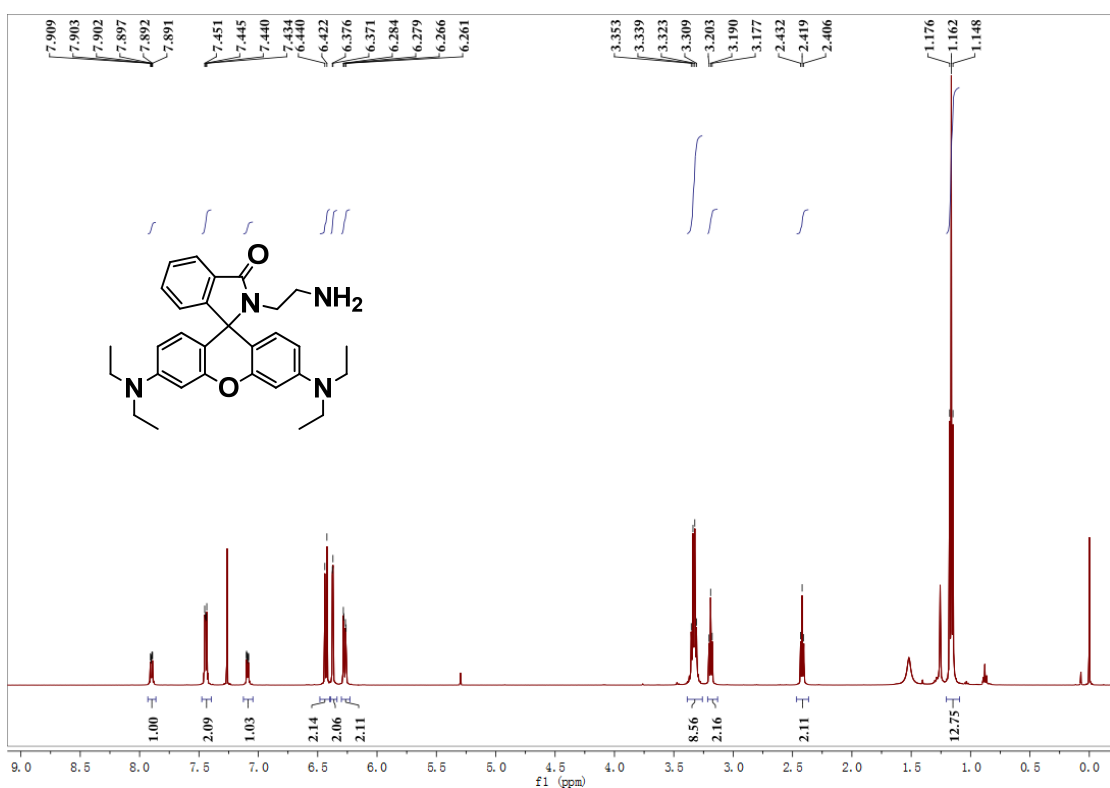


Figure S1. ¹H NMR spectrum of compound 7 (500 MHz, CDCl₃, 298 K).

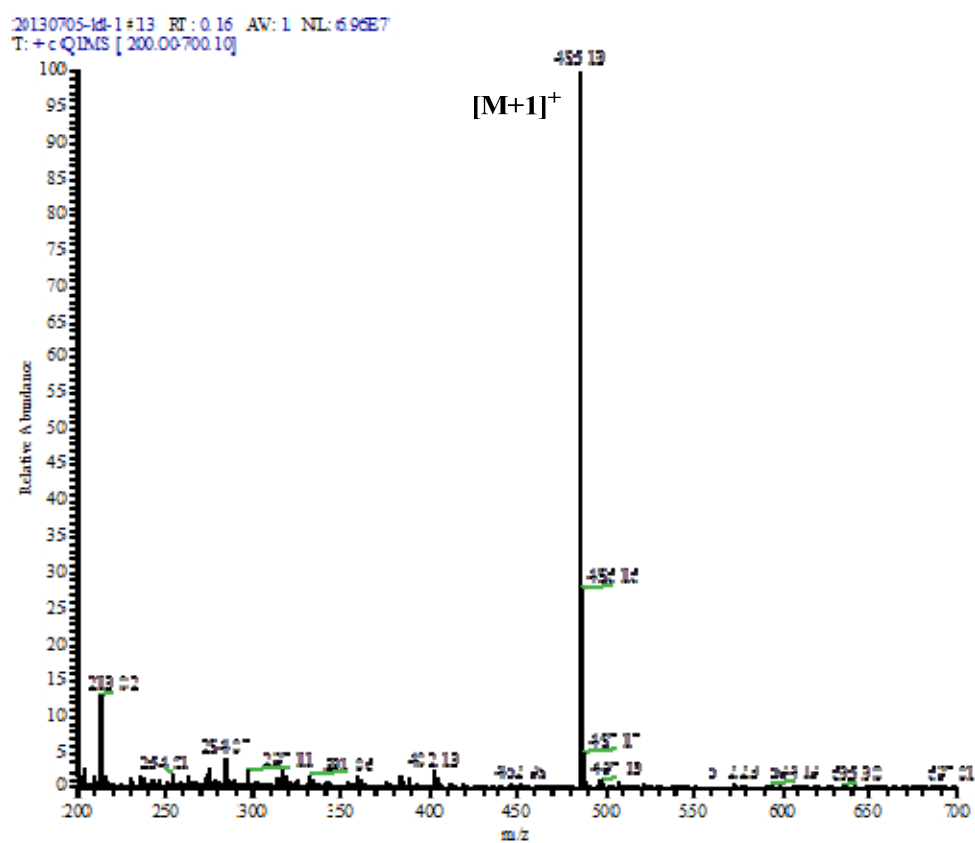
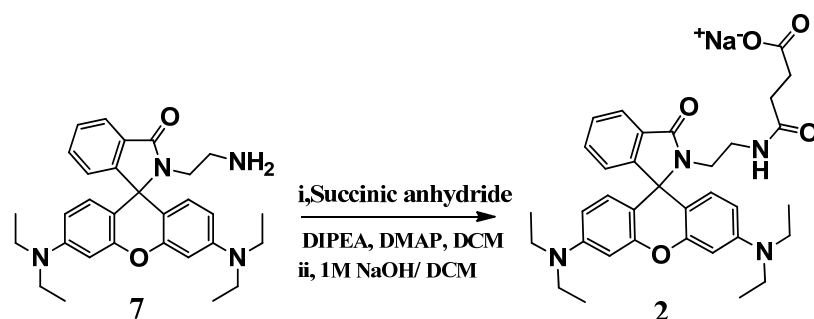


Figure S2. ESI-MS spectrum of compound 7.

Synthesis of 4-((2-(3',6'-bis(diethylamino)-3-oxospiro[isoindoline-1,9'-xanthen]-2-yl)ethyl)amino)-4-oxobutanoic acid (2).



Succinic anhydride (82 mg, 0.8264 mmol) was added to a stirred solution of amine **5** (200 mg, 0.4132 mmol), 4-DMAP (50 mg, 0.4132 mmol) and DIPEA (140 μ L) in 8 mL of dry DCM. Then, the resulting mixture was stirred at room temperature under a nitrogen atmosphere for 16 h. The crude mixture was treated with 1 M NaOH for 30 min followed by extraction with DCM (15 mL x 3 times). The combined organic phase was dried with dry $MgSO_4$ and concentrated in vacuum to remove the DCM solvent to yield a pink residue. The residue was purified on a silica gel column with MeOH/CH₂Cl₂ (v:v 1:20) to afford a pink solid (180 mg, 75% yield). R_f =0.4 (MeOH/CH₂Cl₂: v:v 2:25); ¹H NMR (500 MHz, CDCl₃, 298 K): δ 7.905-7.888(m, 1H), 7.480-7.466(m, 2H), 7.309(s, 1H(CONH)), 7.105-7.088(m, 1H), 6.418-6.379(q, 4H), 6.291-6.268(q, 2H), 3.357-3.268(m, 10H), 3.063-3.035(q, 2H), 2.622-2.596(t, J=6.0 Hz, 2H), 2.484-2.459(t, J=5.5 Hz, 2H), 1.182-1.154(t, J=7.0 Hz, 12H); ¹³C NMR(126 MHz, CDCl₃, 298 K): 175.13, 172.67, 170.15, 153.79, 153.41, 149.12, 133.03, 130.42, 128.49, 128.39, 124.01, 123.01, 108.44, 104.63, 97.94, 66.01, 44.45, 40.56, 40.04, 30.83, 30.39, 12.66; ESI-MS(m/z): calcd for [M-Na]⁻ C₃₄H₃₉N₄O₅⁻ 583.2926, found 583.12, HRMS found 583.2926.

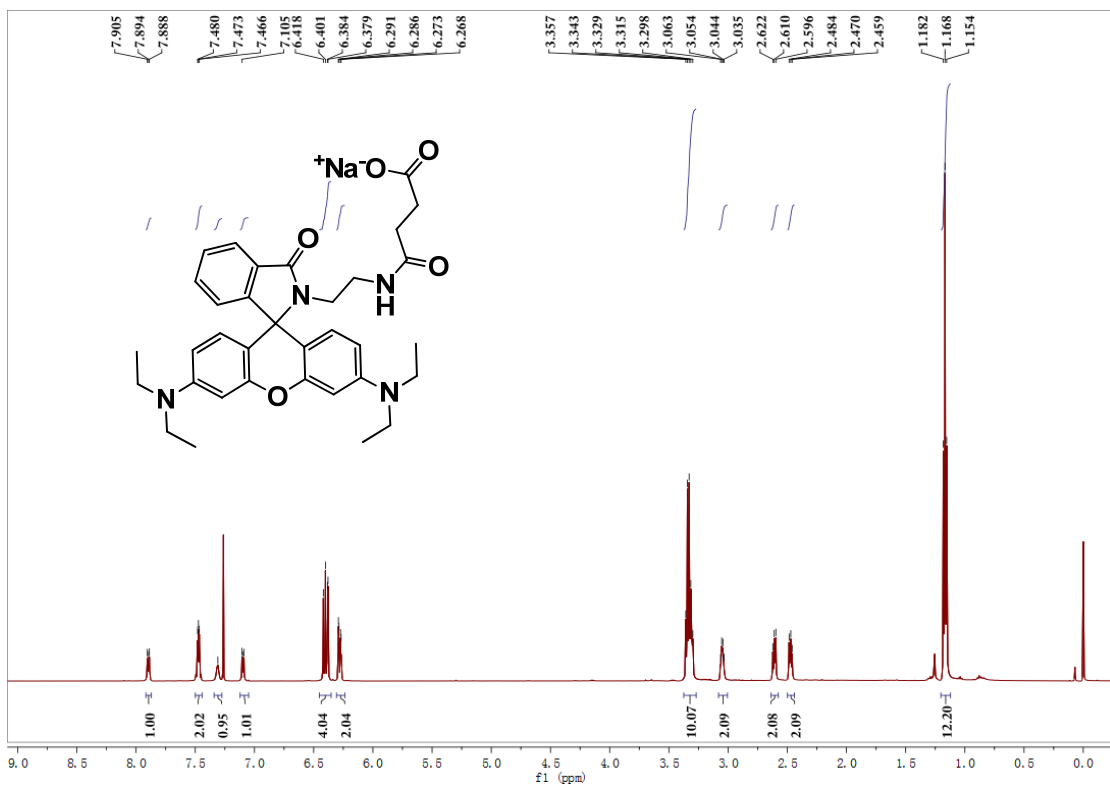


Figure S3. ¹H NMR spectrum of compound 2 (500 MHz, CDCl₃, 298 K).

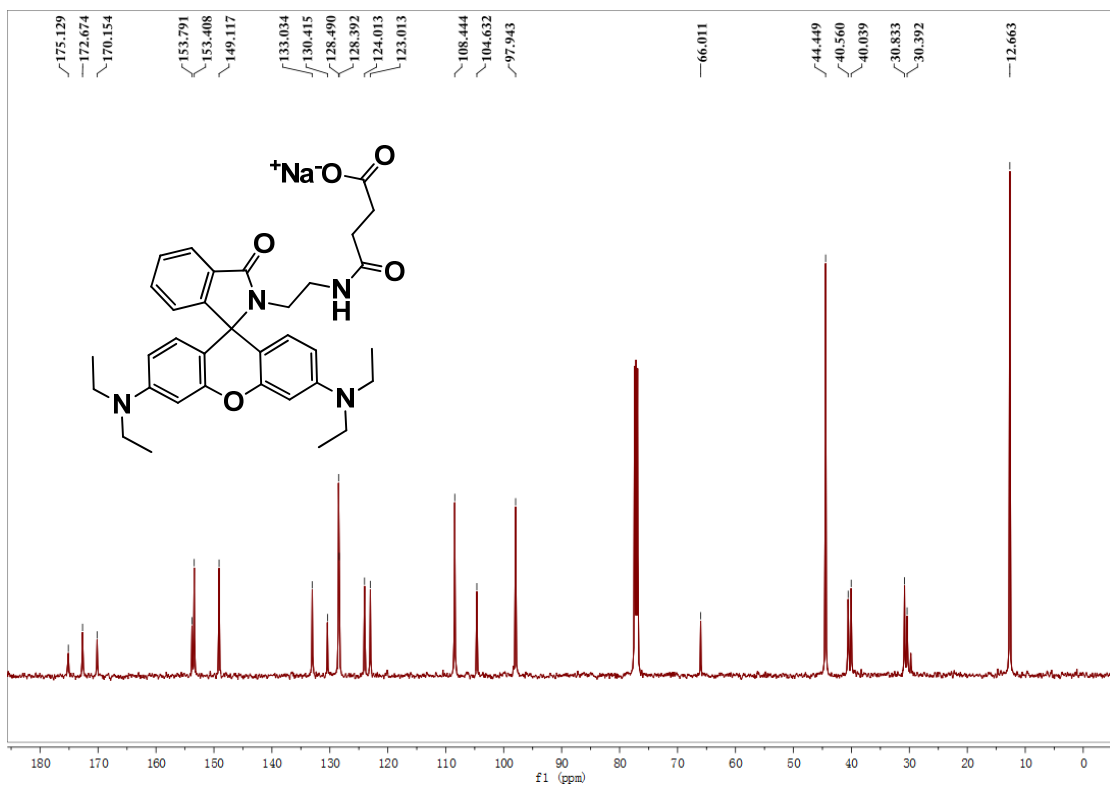


Figure S4. ¹³C NMR spectrum of compound 2 (126 MHz, CDCl₃, 298 K).

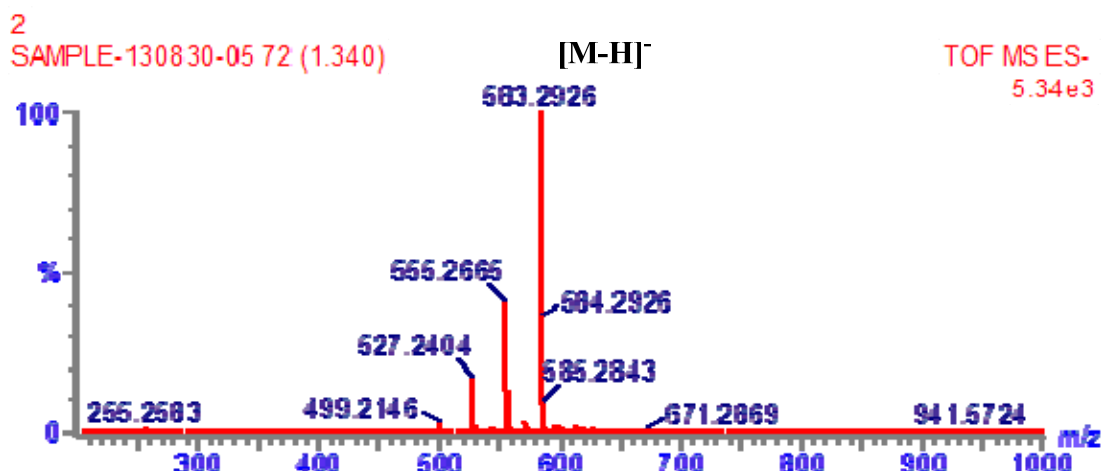
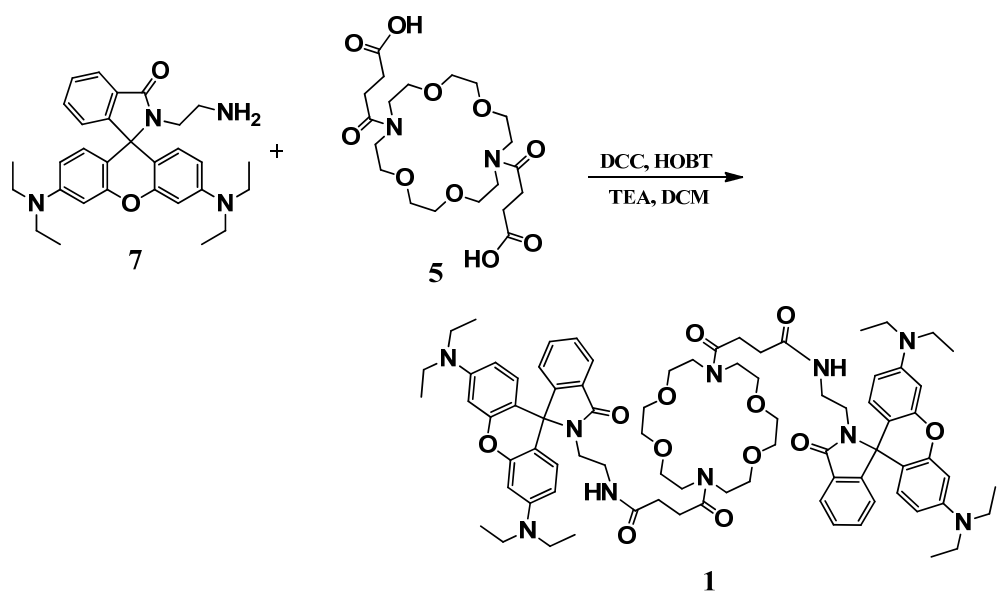


Figure S5. ESI-HRMS spectrum of compound 2.

Synthesis of Rhodamine B-azacrown ether conjugate 1.



To a stirred solution of diacid **5** (88 mg, 0.1908 mmol, which was prepared in the first step), N,N'-methanediylidenedicyclohexanamine (117 mg, 0.5724 mmol, 3 eq.), HOBT (51 mg, 0.3816 mmol, 2 eq.) and DIPEA (66 µL, 2 eq.) in 10 mL of DCM was added amine **7** (203 ng, 0.4198 mmol, 2.2 eq.). Then, the resulting mixture was stirred

at room temperature under a nitrogen atmosphere for 12 h. The progress of the reaction was monitored by TLC. After the crude materials were filtered through a glass frit to remove DCU and concentrated in vacuum to remove the DCM solvent, the residue was further purified on a silica gel column with MeOH/CH₂Cl₂ (v:v 1:20 to 1:10) to afford a pink solid (250 mg, 93% yield). R_f=0.5 (MeOH/CH₂Cl₂: v:v 1:10); ¹H NMR (500 MHz, CDCl₃, 298 K): δ 7.898-7.881(m, 2H), 7.451-7.433(q, 4H), 7.078-7.061(q, 2H), 6.771-6.753(br, 4H), 6.442-6.424(d, 4H), 6.371-6.366(d, 4H), 6.286-6.263(q, 4H), 3.659-3.545(m, 24H), 3.338-3.321(m, 20H), 3.041-3.011(q, 4H), 2.624-2.598(t, J=7.0 Hz, 4H), 2.436-2.409(t, J=7.0 Hz, 4H), 1.176-1.148(t, J=7.0 Hz, 24H); ¹³C NMR(126 MHz, CDCl₃, 298 K): δ 171.05, 168.59, 152.78, 152.27, 147.93, 131.66, 129.59, 127.52, 127.11, 122.85, 121.85, 107.33, 104.01, 96.83, 76.30, 76.04, 75.79, 69.88, 69.71, 69.60, 69.42, 69.23, 68.94, 68.58, 64.47, 47.79, 47.69, 46.19, 43.35, 39.15, 30.91, 30.32, 28.67, 28.34, 27.54, 21.67, 11.59. ESI-MS (m/z): calcd for [M+1]⁺ C₈₀H₁₀₃N₁₀O₁₂⁺ 1395.7751, [M+Na]⁺ C₈₀H₁₀₂N₁₀NaO₁₂⁺ 1417.7571, found 1395.96, 1417.97, HRMS found 1395.7751, 1417.7587.

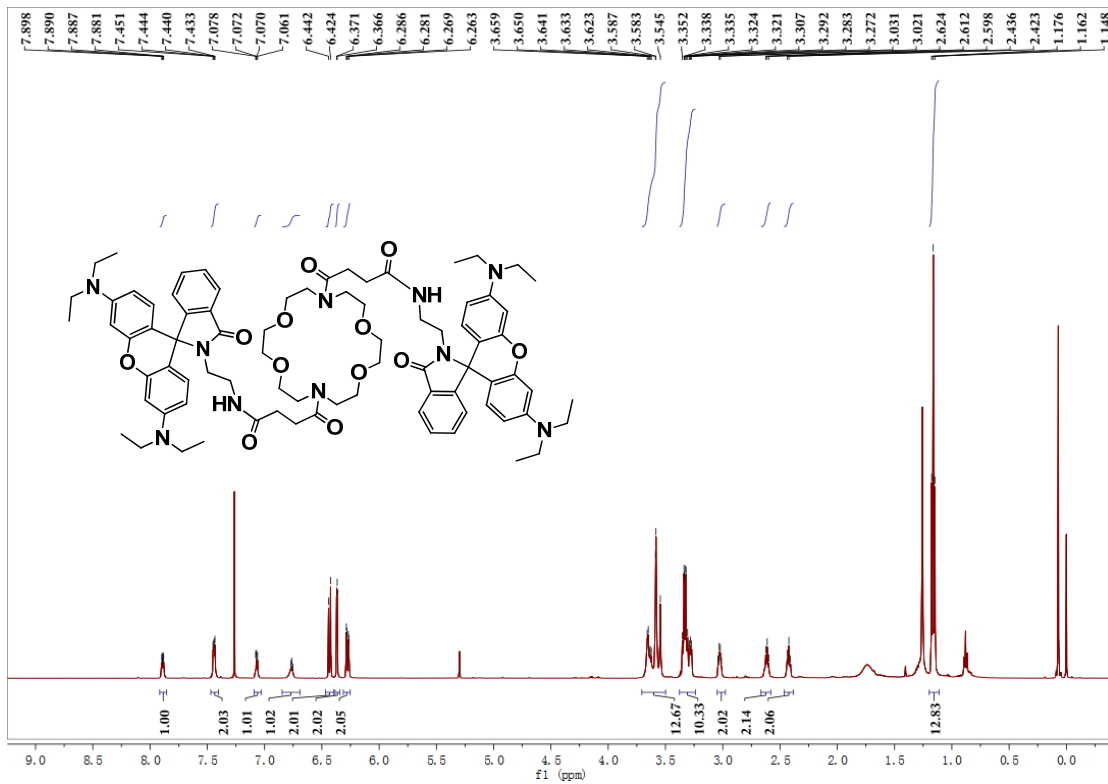


Figure S6. ^1H NMR spectrum of compound **1** (500 MHz, CDCl_3 , 298 K).

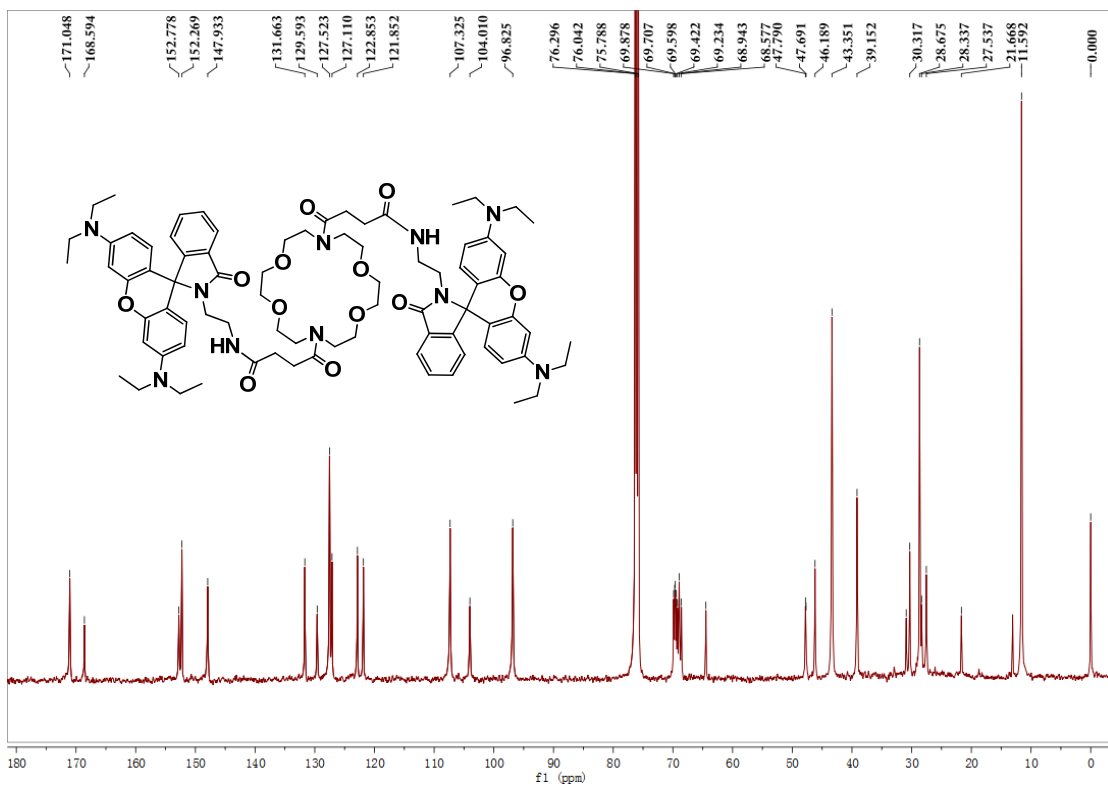


Figure S7. ^{13}C NMR spectrum of compound **1** (126 MHz, CDCl_3 , 298 K).

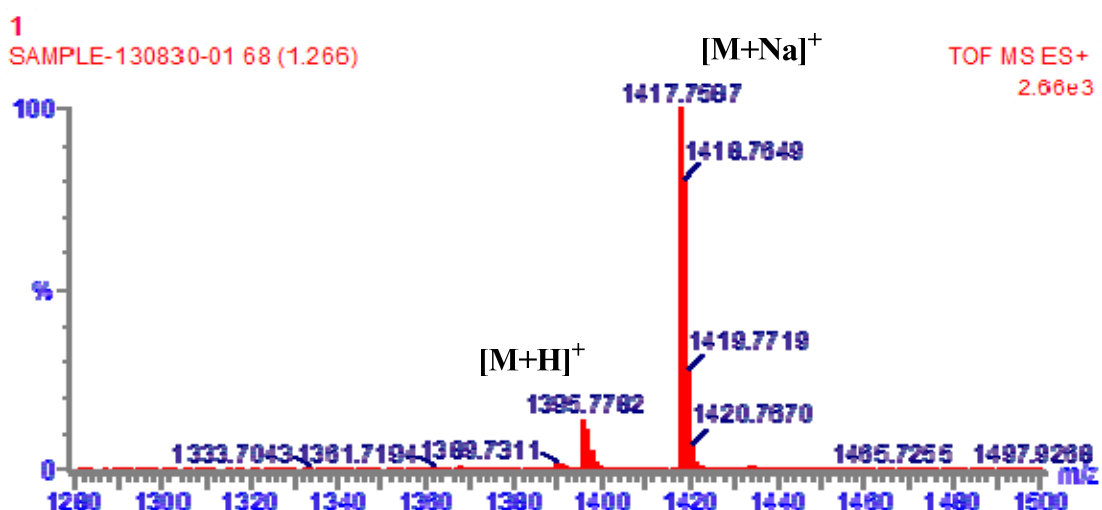


Figure S8. ESI-MS spectrum of compound 1.

3. UV-Vis absorbance and fluorescence experiments of probe 1 and 2.

Stock solutions of the metal salts (i.e., NaCl, KCl, LiCl, CaCl₂, AgNO₃, PbCl₂, BaCl₂, MgCl₂, MnCl₂, FeCl₂, CdCl₂, CrCl₃, NiCl₂, SnCl₂, Pd(OAc)₂, HgCl₂, NH₄Cl, CoCl₂) (12 mM) were prepared in methanol/H₂O (3:2, v/v). The stock solutions of probe **1** (20 μ M) and **2** (40 μ M) were prepared in methanol/H₂O (3:2, v/v, pH 7.2). For all of the fluorescence spectra, the excitation and emission wavelengths were 555 and 582 nm, respectively. UV-Vis absorbance and fluorescence experiments were performed using a 20 μ M solution of probe **1** and a 40 μ M solution of probe **2** in methanol/H₂O (3:2, v/v, pH 7.2) and various cations solution (12 mM) in methanol/H₂O (3:2, v/v)

Fluorescence spectra of probe **1 in the presence of different amounts of Cr³⁺.**

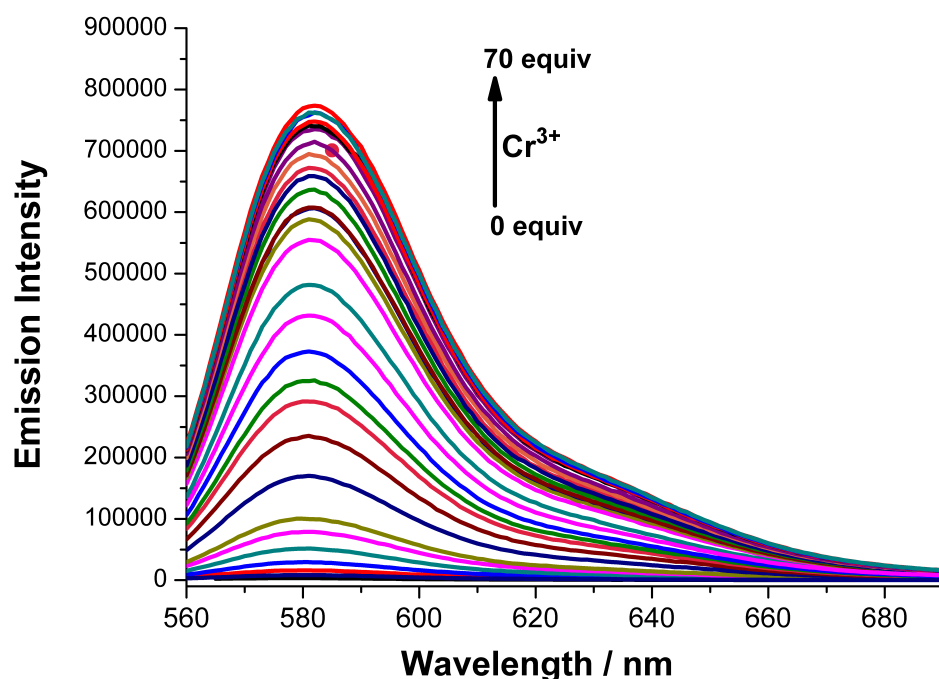


Figure S9. Fluorescence spectra of probe **1** (20 μM) upon addition of different amounts of Cr³⁺ in a methanol/H₂O (3:2, v:v, pH 7.2) solution. The excitation and emission wavelengths were 555 and 582 nm, respectively. Slit: 2.5 nm / 2.5 nm. A more than 50-fold fluorescence enhancement was observed under saturated conditions.

Color change of probe **1 in the presence of different amounts of Cr³⁺.**



Figure S10. Color change of probe **1** (20 μM) in a methanol/H₂O (3:2, v:v, pH 7.2) solution upon addition of different amounts of Cr³⁺ (Free, 0.5, 1.0, 2.0, 5.0, and 10 equiv.) demonstrating that **1** can serve as a “naked-eye” probe for Cr³⁺ (maintained for 1 hour after the addition).

Job's Plot of probe **1 with Cr³⁺**

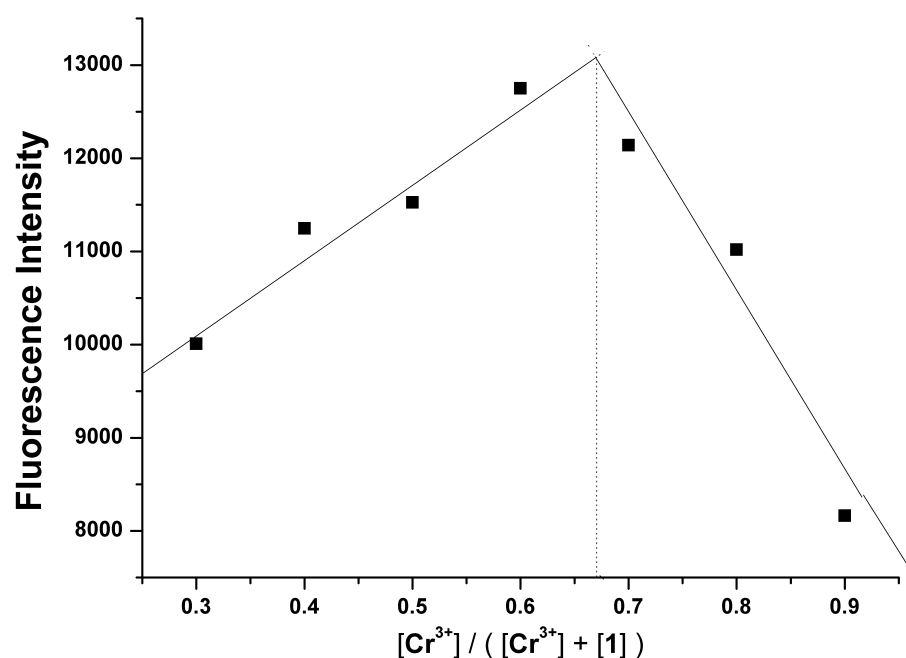


Figure S11. Job's plot of probe **1** indicating the bonding of **1** towards Cr³⁺. Total concentration of **1** plus Cr³⁺ ion is 20 μM . The excitation and detection wavelengths

were 555 and 582 nm, respectively. Slit: 4.5 nm/4.5 nm.

Determination of the association constant K_a .

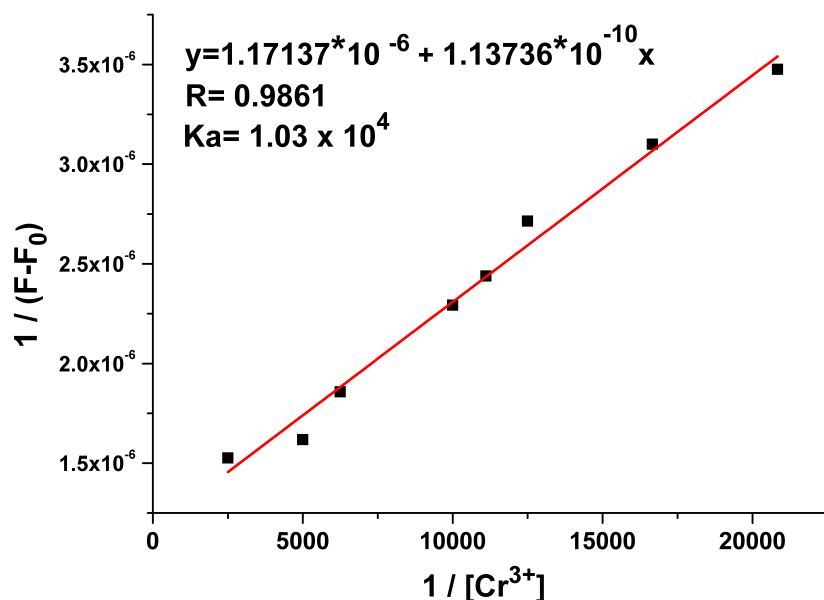


Figure S12. Association constant of probe **1** with Cr^{3+} (1:2) with error bars that display three standard deviations. The excitation and emission wavelengths were 555 and 582 nm, respectively. Slit: 2.5 nm / 2.5 nm.

Determination of the association constant: According to the titration experiment, the apparent association constant was determined using the following formula: $F - F_0 = \Delta F = [\text{Cr}^{3+}] (F_{\max} - F_0) / (K_a + [\text{Cr}^{3+}])$, where F is the obtained fluorescence intensity, F_{\max} is the saturated fluorescence intensity for complex **1**- Cr^{3+} , and F_0 is the fluorescence intensity of free probe **1**. When the reciprocal of ΔF is plotted as a function of Cr^{3+} concentration, a linear relationship was obtained ($y = A + Bx$). K_a was calculated from A / B . Therefore, K_a is 1.03 M^{-1} , as shown in **Figure S12**.

Determination of detection limit.

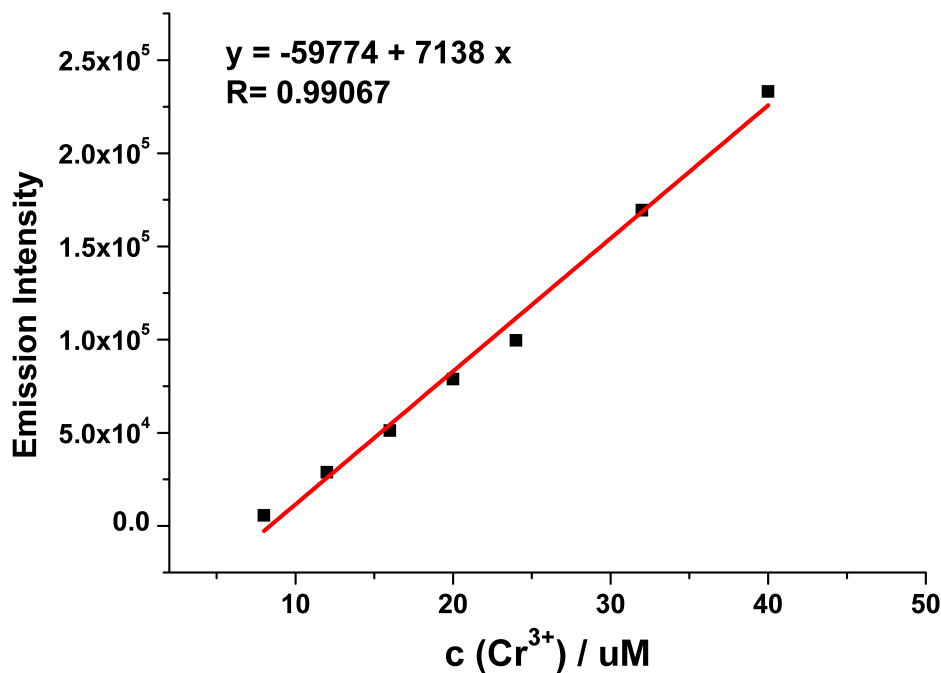


Figure S13. Fluorescence intensity at 582nm of **1** (20μM) as a function Cr³⁺ concentration. The excitation wavelength was 555, Slit: 2.5 nm / 2.5 nm.

Determination of the detection limit:

The detection limit DL of probe **1** for Cr³⁺ was determined from the following equation: $DL = K * (SD/S)$

Where K = 2 or 3 (We take 2 in this case); SD is the standard deviation of the blank solution; S is the slope of the calibration curve.

SD value calculated from standard deviation of the blank solution (probe **1** (20 μM) in a methanol/H₂O (3:2, v:v, pH 7.2)) is 514. From **Figure S13** we get slope = 7138. Thus, using the formula we get the Detection Limit = 0.144μM (7.5 ppb).

Color change of probe 1 in the presence of various cations.



Figure S14. Color change of probe 1 (20 μM) in a methanol/H₂O (3:2, v:v, pH 7.2) solution upon addition of 5 equiv. of various cations (maintained for 1 hour after the addition). As shown in **Figure S14**, the addition of Cr³⁺ significantly changed the color of the solution from colorless to bright pink.

Change in the ratio of probe 1with background cations in in the presence of Cr³⁺.

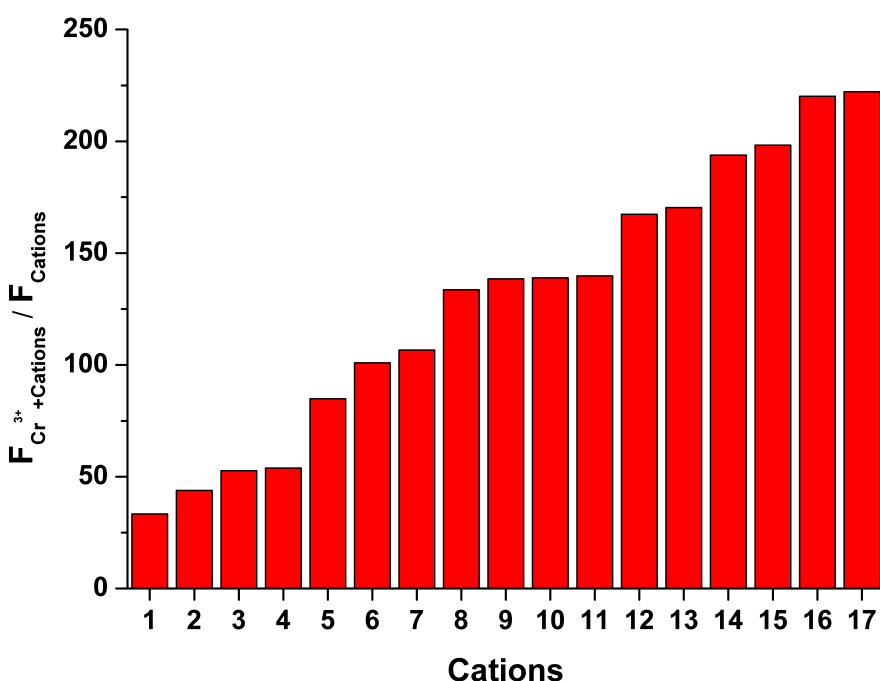


Figure S15. Change in the ratio ($F_{Cr^{3+} + \text{Cations}} / F_{\text{Cations}}$) of the fluorescence intensity of probe **1** (20 μM) at 582 nm upon addition of 5 equiv. of Cr^{3+} ion in the presence of 5 equiv. of background cations (i.e., 1-Pd²⁺, 2-Sn²⁺, 3-Pb²⁺, 4-Ca²⁺, 5-Mn²⁺, 6-Cd²⁺, 7-Cu²⁺, 8-Hg²⁺, 9-Ni²⁺, 10-Fe²⁺, 11-Co²⁺, 12-Zn²⁺, 13-Mg²⁺, 14-NH₄⁺, 15-Na⁺, 16-K⁺, 17-Li⁺). The excitation wavelength is 555 nm. Silt: 2.5 nm / 2.5 nm. As shown in **Figure S15**, the addition of Cr^{3+} can markedly influence the fluorescence intensity resulting from subsequent addition of other cations, which indicated that probe **1** is an excellent selective chemosensor for the Cr^{3+} ion.

UV-Vis spectra of probe 1 in the presence of various cations.

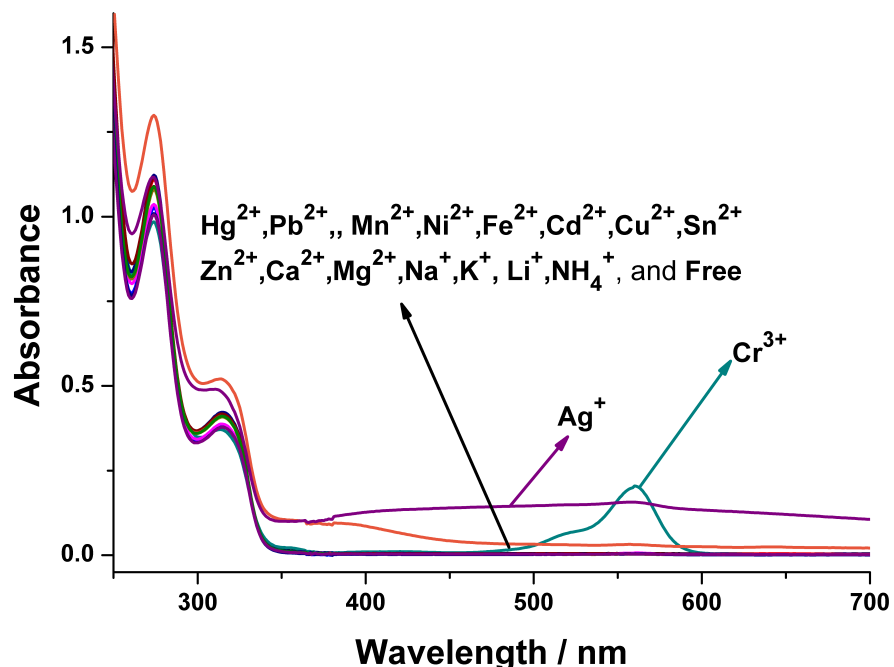


Figure S16. UV-Vis absorbance spectra of probe 1 (20 μM) in the presence of different cations (5 equiv.). As shown in **Figure S16**, the solution of probe 1 upon addition of the Cr³⁺ ion exhibited a strong absorption intensity at 562 nm (olive-green line) and the addition of Ag⁺ exhibited a strong and mild absorption intensity from 350 to 700 nm (purple line), which is due to the formation of a AgOH precipitate. Except for 562 nm, two new absorption band centered at 274 and 315 nm appeared with decreasing intensity.

Comparison of fluorescence spectra of probe 1 with probe 2 in the presence of various cations.

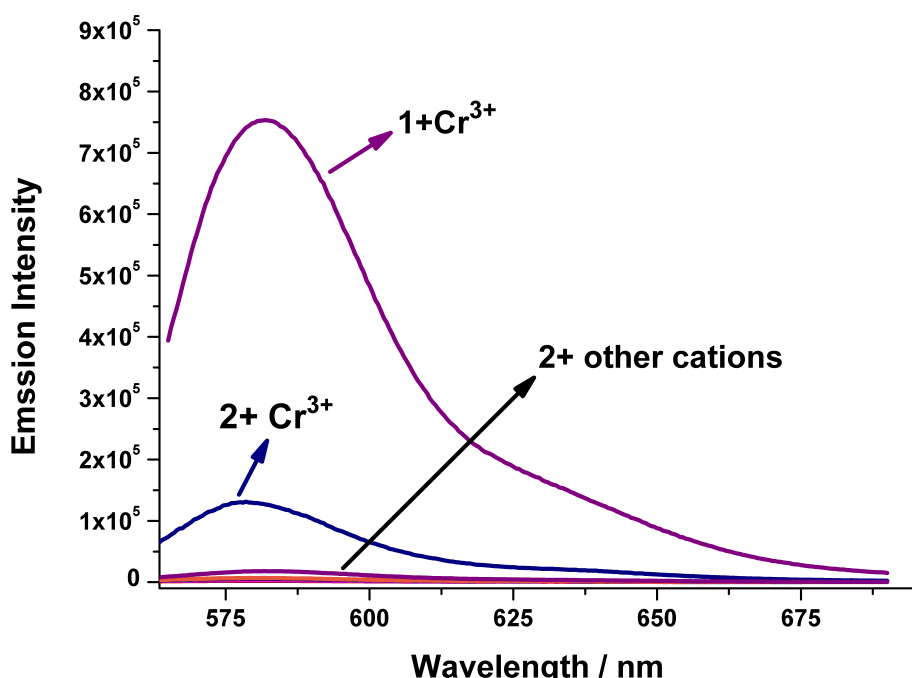


Figure S17. Comparison of the fluorescence intensity of probe **1** ($20 \mu\text{M}$) upon addition of Cr^{3+} (5 equiv.) and probe **2** ($40 \mu\text{M}$) upon addition of various cations ($40 \mu\text{M}$). As shown in **Figure S17**, probe **2** displayed a better response to Cr^{3+} (blue line). However, its fluorescence intensity is much less than probe **1** (purple line) under the same conditions. The results from **Figure S17** combined with those in **Figure 5** indicate that the azacrown ether unit of probe **1** played a key role in improving its sensibility and selectivity towards Cr^{3+} ion.

Comparison of Partial ^1H NMR of probe 1 with or without Cr^{3+} .

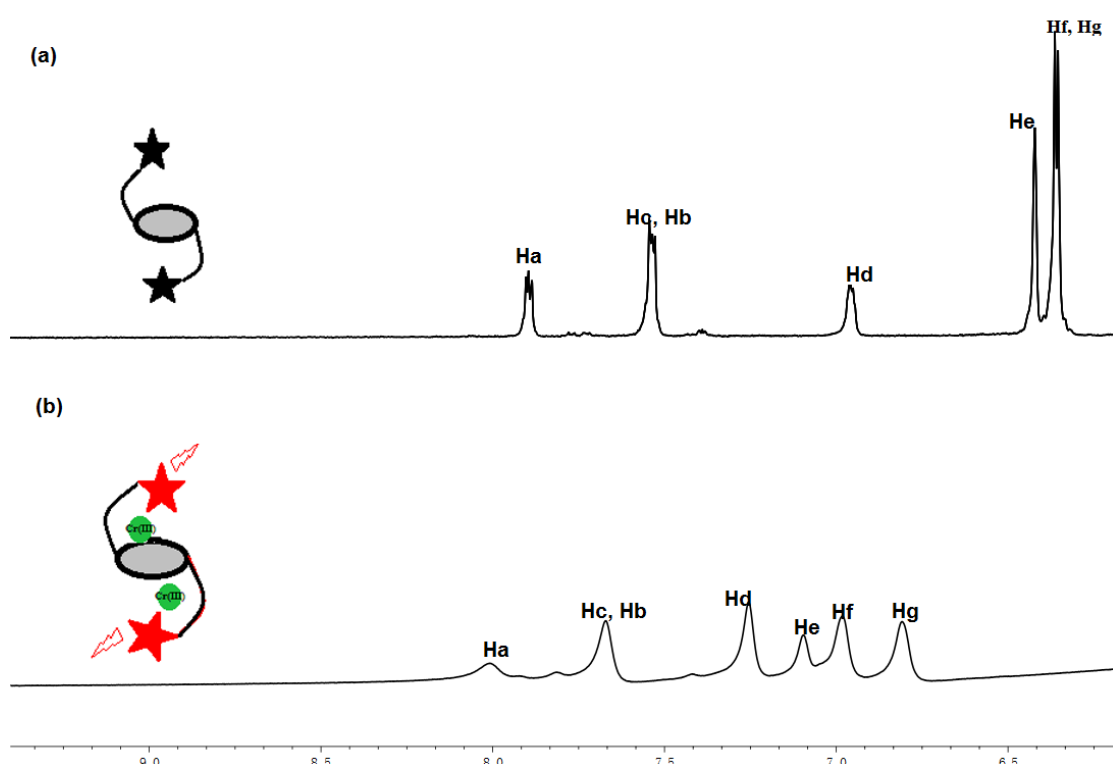


Figure S18. Partial ^1H NMR spectra (500 MHz, 298 K, $\text{CD}_3\text{OD}/\text{D}_2\text{O}$ (v:v 3:2)) of (a) probe 1 and (b) probe 1 + 5 equiv of Cr^{3+} . All of the atom labels are shown in **Scheme 2**. In comparison to probe 1 without the addition of Cr^{3+} , the Hd, He, Hf and Hg peaks are markedly shifted downfield.

pH response of Probe 1

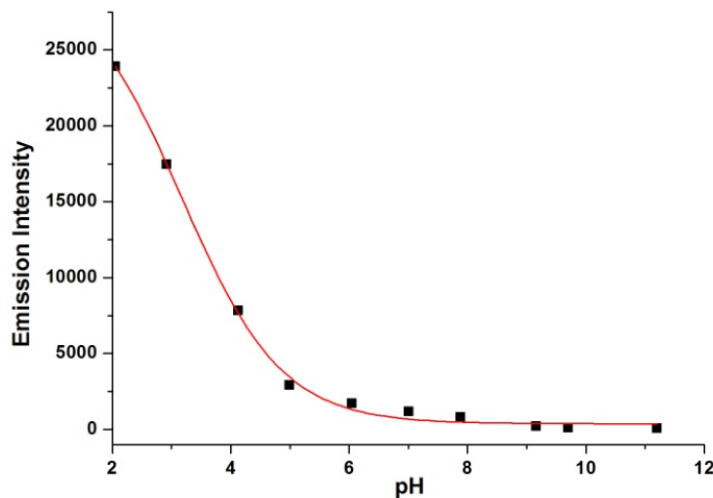


Figure S19. The influence of pH on the fluorescence of probe **1** (20 μM) in MeOH/H₂O solution (3:2, v/v), the pH was modified by adding 10% HCl or 10% NaOH. Excitation was performed at 555 nm.

Table S1. Comparison of the present method with other reported Cr³⁺ selective fluorescence sensor.

| Type of Chemosensors | Selectivity | Association constant / binding Constant for Cr ³⁺ | Detection of Limit for Cr ³⁺ | References |
|--|--|--|---|-----------------|
| Turn on-based on Rhodamine B and aza-crown Conjugate | Cr ³⁺ in a methanol/water solution (3:2, v:v, pH 7.2) | $K_a=1.03\times 10^4 \text{ M}^{-1}$ | 7.5 ppb (0.144 μM) | Sensor 1 |
| Turn on-based on Rhodamine 6G derivatized with quinoline | Hg ²⁺ and Cr ³⁺ in an acetonitrile/HEPES buffer medium of pH 7.3 | $K_a=2.1\times 10^3 \text{ M}^{-1}$ | 5.6 ppm | 1 |
| Turn on-based on DTNBA -modified gold nanoparticles | Cr ³⁺ in a HEPES buffer (pH 7.5). | - | 93.6 ppb | 2 |
| Turn off-based on 9-Acridone-4-carboxylic acid | Cr ³⁺ in DMF/water (9:1,v/v) solution | $K_a=8.1378\times 10^4 \text{ M}^{-1}$ | 9.0 μM | 3 |
| FRET-based Rhodamine B and a naphthalimide conjugate | Cr ³⁺ in ethanol/water (2 : 1, v/v) | $K_a=9.4\times 10^3 \text{ M}^{-1}$ | - | 4 |

| | | | | |
|---|--|--|--------------------|-----------|
| Turn on-based on rhodamine 6G with diethylenetriamine/triethylenetetraamine | Fe^{3+} and Cr^{3+} in aqueous solution | $K_a = 4.16 \times 10^4 \text{ M}^{-1}$ | - | 5 |
| Turn on-based on Dansyl-based fluorescent chemosensors | Cr^{3+} in (DMF /H ₂ O (9:1, v/v) | $K_{ass} = 6.07 \pm 0.10 \times 10^7 \text{ M}^{-2}$ | - | 6 |
| Turn on-based on naphthalene derivative | Cr^{3+} in aqueous methanol | $K = 1.027 \times 10^3 \text{ M}^{-1/2}$ | 0.15 μM | 7 |
| Turn on-based on Thiophene anchored coumarin derivative | Cr^{3+} in CH ₃ CN/HEPES buffer(0.02 M, pH 7.4)(4:6, v/v) medium | $K_a = 8 \times 10^4 \text{ M}^{-1}$ | 1.0 μM | 8 |
| Turn on-based on Anthracene appended coumarin derivative | Cr^{3+} in acetonitrile and Methanol/medium | $K_a = 1.1 \times 10^5 \text{ M}^{-1}$ | 0.5 μM | 9 |
| Turn on-based on benzimidazole derivatives | Cr^{3+} and Fe^{3+} in aqueous solution | $K_a = 1.75 \times 10^3 \text{ M}^{-1}$ | 25 μM | 10 |
| Turn on-based on fluorogenic sensor (L1) | $\text{Hg}^{2+}/\text{Cr}^{3+}$ in a neutral water | $K_a = 6.54 \times 10^4 \text{ M}^{-1}$ | - | 11 |
| Turn on-based on phenanthrene-based bis-oxime | Fe^{3+} and Cr^{3+} in a DMSO/MeOH (9:1). | - | 400 μM | 12 |
| FRET-based on Rhodamine-6G derivatized with glutathione | Cr^{3+} in a NaAc-HAc buffer solution (pH 6.0) | $K_{ass} = 3.96 \times 10^5 \text{ M}^{-2}$ | <0.1ppm | 13 |
| FRET-based rhodamine B deterivativated FD8 | Cr^{3+} in ethanol-water (2:1, v/v) solution | $K_a = 9.9 \times 10^3 \text{ M}^{-1}$ | 1 μM | 14 |

Reference

1. Saha, S.; Mahato, P.; G, U. R.; Suresh, E.; Chakrabarty, A.; Baidya, M.; Ghosh, S. K.; Das, A., Inorg. Chem. **2012**, 51, 336.
2. Dang, Y. Q.; Li, H. W.; Wang, B.; Li, L.; Wu, Y., ACS applied materials & interfaces **2009**, 1, 1533.
3. Karak, D.; Banerjee, A.; Sahana, A.; Guha, S.; Lohar, S.; Adhikari, S. S.; Das, D., J. Hazard. Mater. **2011**, 188, 274.
4. Zhou, Z.; Yu, M.; Yang, H.; Huang, K.; Li, F.; Yi, T.; Huang, C., Chem. Commun. **2008**, 44, 3387.
5. Mao, J.; Wang, L.; Dou, W.; Tang, X.; Yan, Y.; Liu, W., Org. Lett. **2007**, 9, 4567.
6. Wu, H.; Zhou, P.; Wang, J.; Zhao, L.; Duan, C., New J. Chem. **2009**, 33, 653.
7. Das, S.; Sahana, A.; Banerjee, A.; Lohar, S.; Guha, S.; Matalobos, J. S.; Das, D., Anal. Methods **2012**, 4, 2254.
8. Guha, S.; Lohar, S.; Banerjee, A.; Sahana, A.; Hauli, I.; Mukherjee, S. K.; Matalobos, J. S.; Das,

- D., *Talanta* **2012**, 91, 18.
9. Guha, S.; Lohar, S.; Banerjee, A.; Sahana, A.; Mukhopadhyay, S. K.; Matalobos, J. S.; Das, D., *Anal. Methods* **2012**, 4, 3163.
10. Wang, M.; Wang, J.; Xue, W.; Wu, A., *Dyes and Pigments* **2013**, 97, 475.
11. Das, P.; Ghosh, A.; Bhattacharyya, H. and Das, A., *RSC Adv.* **2012**, 2, 3714.
12. Bravo, V.; Gil, S.; Costero, A. M.; Kneeteman, M. N.; Llaosa, U.; Mancini, P. M. E.; Ochando, L. E.; Parra, M., *Tetrahedron* **2012**, 68, 4882.
13. Hu, X.; Zhang, X.; He, G.; He, C.; Duan, C., *Tetrahedron* **2011**, 67, 1091.
14. Wan, Y.; Guo, Q.; Wang, X.; Xia, A., *Analytica chimica acta* **2010**, 665, 215.